ChemComm

COMMUNICATION

View Article Online
View Journal | View Issue

Published on 26 April 2017. Downloaded by University of California - San Diego on 29/05/2017 12:10:43.

Check for updates

Cite this: *Chem. Commun.*, 2017, 53, 5629

Received 27th March 2017,
Accepted 26th April 2017

DOI: 10.1039/c7cc02304a

rsc.li/chemcomm

TTE DNA–Cu NPs: enhanced fluorescence and application in a target DNA triggered dual-cycle amplification biosensor†

Guangfeng Wang,* Jing Wan and Xiaojun Zhang *

A crowded TTE DNA structure for the preparation of Cu NPs with enhanced fluorescence was prepared and applied for the ultrasensitive detection of target DNA.

Biotemplated metallization has drawn increasing attention for the construction of nanoscale assemblies and hybrid structures because of their specific applications in fluorescence, catalysis, biological labeling and optical sensing.[1] Due to its unique nanosized structure, excellent programmable properties, and rich functional groups including heterocyclic nitrogen atoms, amino groups, and phosphate groups, deoxyribonucleic acid (DNA) represents a particularly good biotemplate candidate, which can bind with specific metal ions and provide nucleation sites for the growth of metallic nanoparticles. Recently, DNA templated fluorescent nanomaterials as sensitive reporters have been investigated, such as DNA templated-gold nanoclusters (Au NCs),[2] -silver nanoclusters (Ag NCs)[3] and -Cu nanoparticles (Cu NPs).[4] Among them, DNA-templated Cu NPs (DNA–Cu NPs) have attracted considerable attention as fluorescent probes in biosensing for the advantages of label-free operation, good biocompatibility, low-cost, ease of preparation, low-toxicity and excellent fluorescence properties.[5] Since the discovery of fluorescent DNA–Cu NPs in 2010,[4a] the fluorescent DNA–Cu NPs have gained much progress and fall into two major categories according to the DNA template used. The first one is double stranded DNA–Cu NPs (ds DNA–Cu NPs) first prepared by Mokhir *et al.*[4a] They used random ds DNA as an efficient template to prepare fluorescent Cu NPs with a low concentration of $CuSO_4$. Thereafter, several research studies on fluorescent Cu NPs with various ds DNA templates to enhance the fluorescence have been reported. By introducing the rolling circle amplification (RCA) mechanism, Wang and co-workers developed a novel long concatemeric ds DNA as a template for the preparation of Cu NPs with enhanced fluorescence properties, which were further applied to detect microRNA.[6] By combining with the hybridization chain reaction (HCR), another novel long chain ds DNA as a template for fluorescent Cu NPs was explored, and the fluorescence has been efficiently amplified for label-free and ultrasensitive sensing of a series of analytes.[7] Further, Qu's group has successfully applied the fluorescence enhanced Cu NPs on HCR engineered ds DNA templates in a novel enzyme-free amplified platform for the selective and quantitative detection of cancer cells and microRNA.[8] Besides elongation of the chain length of ds DNA, the regulation of the sequences to enhance the fluorescence of Cu NPs has also been studied. Ouyang's group in 2015 discovered that, compared with random ds DNA, increasing the pairs of adenine–thymine (AT) sequences could enhance the fluorescence of the ds DNA–Cu NPs.[9] Despite the development of Cu NPs with various ds DNA templates including random-, RCA-, HCR-, AT base-based ds DNA, *etc.*, the enhancement of the fluorescence efficiency of ds DNA–Cu NPs is still limited.

The second category of fluorescent DNA–Cu NPs is templated on single stranded DNA (ss DNA) with polythymine (polyT), first developed by Wang and co-workers in 2015.[10] They proposed a novel single strand polyT ss DNA template, realizing the controllable preparation of Cu NPs in which the size of Cu NPs was dependent on the length of polyT. The polyT ss DNA templated Cu NPs (polyT–Cu NPs) exhibit more highly efficient fluorescence and their mega-Stokes shift was more advantageous for the removal of interference from background signals of the complex source than ds DNA–Cu NPs.[9] Based on the results of Wang's group, the vast majority of research focuses on the exploration of polyT–Cu NPs as fluorescent probes in biosensors. For example, Qing's group developed a novel fluorescence strategy for a hydrogen peroxide assay using polyT–Cu NPs as probes.[11] Ou's group reported polyT–Cu NPs as effective fluorescent probes to develop a simple and sensitive fluorescence assay for trypsin, cytochrome *c* (Cyt *c*) and Pb^{2+}.[12] Wang's group also proposed polyT–Cu NPs as fluorescent probes for thiol-containing drug, Hg(II) ion and protein detection.[13] A very recent study and application of the polyT–Cu NP probe also included the sensing of alkaline phosphatase (ALP) in real samples by Dai's group.[14] (The development and application of fluorescent ds DNA or polyT ss DNA templated Cu NPs are summarized in Table S1 (ESI†).)

Anhui Key Laboratory of Chem-Biosensing, College of Chemistry and Materials Science, Center for Nanoscience and Nanotechnology, Anhui Normal University, Wuhu, 241000, P. R. China. E-mail: wangyuz@mail.ahnu.edu.cn; Fax: +86-553-3869303; Tel: +86-553-3869303

† Electronic supplementary information (ESI) available: Experimental details, control experiments and optimization of the conditions. See DOI: 10.1039/c7cc02304a

Published on 26 April 2017. Downloaded by University of California - San Diego on 29/05/2017 12:10:43.

Generally, these works utilized the excellent fluorescence properties of polyT–Cu NPs to fabricate a series of novel biosensors. However, little work has been reported on strengthening the fluorescence intensity of polyT–Cu NPs, except for a recent work of Lu's group in 2016.[15] In their work, to increase the efficiency of fluorescent polyT–Cu NPs, they explored a novel hairpin DNA as a template which is a "hybrid" of ds DNA and polyT ss DNA. Despite the improvement of the fluorescence of Cu NPs at 615 nm, which may have originated from polyT–Cu NPs, there existed some limitations such as the effect of fluorescence at 580 nm from ds DNA–Cu NPs and the embarrassment of different incubation times of ds DNA and ss DNA templated Cu NPs. Thus, it is necessary to develop a novel strategy to enhance the fluorescence of polyT–Cu NPs.

Considering that until now most reported fluorescence enhancement of the DNA–Cu NPs has been realized by extending the chain of the DNA template while not in view of the DNA structure, it is desirable and challenging to explore a novel DNA structure for favorable growth of polyT–Cu NPs to further enhance the fluorescence intensity.

The molecular crowding effect, which is important in biology and biotechnology, on many biochemical reactions has been investigated.[16] There is increasing evidence that the molecular crowding environment has significant effects on the diffusion rate, hybridization efficiency, folded structure, structural stability and interactions of nucleic acids.[17] Recently, Qu *et al.* have studied the impact of molecular crowding with polyethylene glycol (PEG) acting as a crowding reagent on the synthesis of fluorescent DNA–Ag NCs. Although the molecular crowding could enhance the fluorescence of DNA–Ag NCs by one order of magnitude, the crowding environment created by the external reagent made the process complex. It inspired us to speculate the question: why not create a crowding environment by regulating the DNA spatial structure to prepare fluorescence enhanced DNA–Cu NPs?

Herein, we first developed a crowded polyT DNA structure as a template for the preparation of fluorescence enhanced Cu NPs. The crowded DNA scaffold (polyT DNA tied at two ends, TTE DNA) was composed of two polyT ss DNA which can hybridize with each other to form a double-helical DNA at two ends. It may help in creating a crowded space for the growth of Cu NPs. A graphical representation of TTE DNA templated Cu NPs (TTE DNA–Cu NPs) is illustrated in Scheme 1. Both nucleic acids (termed DNA 1 and 2) contained three regions. Domains a and b in DNA 1 (the names of the oligonucleotides are given in Table S2 (ESI†)) were complementary to domains a* and b* in nucleic acid 2. The regions of polyT sequences, in the middle parts of DNA 1 and 2 (domains c and c*), respectively, were designed as specific regions for the growth of Cu NPs. In addition, in order to compare with TTE DNA–Cu NPs, DNA 1 was used to prepare 1 templated Cu NPs (**1**–Cu NPs) under the same conditions. It was found that TTE DNA–Cu NPs exhibited a strongly red fluorescence and the fluorescence intensity was twice higher than **1**–Cu NPs, which we described as "one plus one is greater than two". (The TTE DNA structure and DNA 1 were also analyzed by NUPACK.[18])

Since DNA templates with different conformations (TTE and polyT) play an important role in the synthesis of Cu NPs, circular dichroism (CD) spectra and gel-electrophoresis were carried out to gain insight into the DNA templates. As shown in Fig. 1A, the

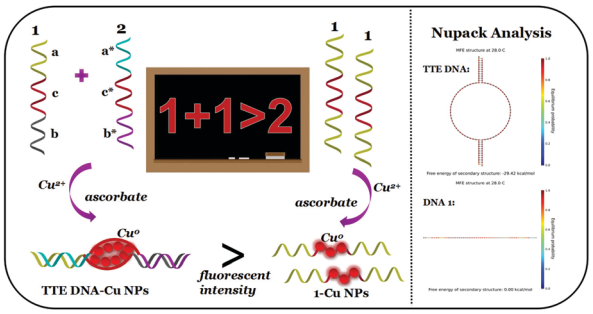

Scheme 1 Schematic representation (left) and NUPACK (right) analysis of the TTE DNA–Cu NPs and **1**–Cu NPs.

ellipticity of TTE DNA–Cu NPs (curve a) at 300 nm was more negative compared with **1**–Cu NPs (curve b), indicating the formation of a rigid structure of the TTE DNA template. The gel-electrophoresis results (Fig. 1B) showed that TTE DNA–Cu NPs (lane a) moved significantly more slowly than 1–Cu NPs (lane b), maybe ascribed to the existence of ds DNA in TTE DNA. Consequently, according to the results of CD spectra and gel-electrophoresis, TTE DNA and DNA 1 possessed different structures to grow Cu NPs as we designed.

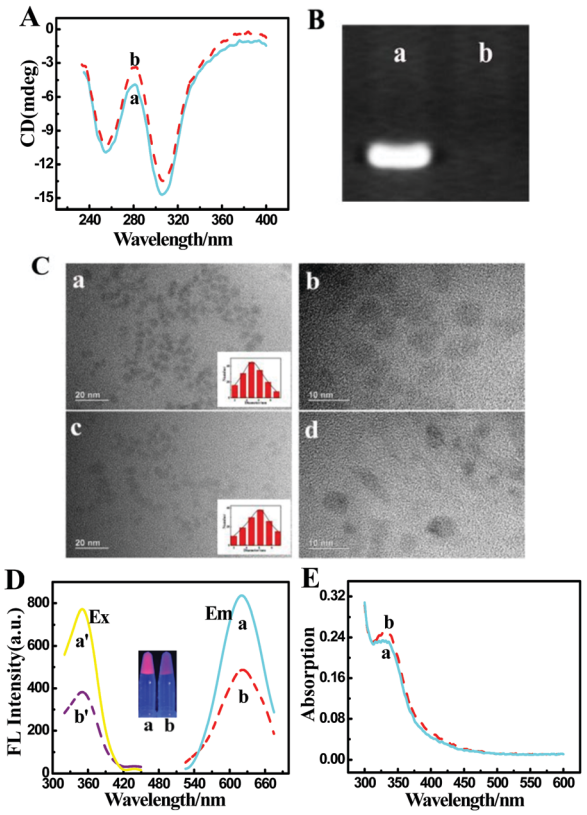

Fig. 1 CD investigation (A) and agarose gel electrophoresis image (B) of TTE DNA–Cu NPs (a) and **1**–Cu NPs (b); (C) TEM images of TTE DNA–Cu NPs (a and b) and **1**–Cu NPs (c and d) at different magnifications (insets: diameter scale size distribution analysis). Fluorescence excitation (a′ and b′) (λ_{ex} = 340 nm)/emission (a and b) (λ_{em} = 615 nm) spectra (inset: the fluorescent Cu NPs generated under UV-light excitation) (D) and UV-vis absorption spectrum (E) of TTE DNA–Cu NPs (a) and **1**–Cu NPs (b).

 This journal is © The Royal Society of Chemistry 2017

Published on 26 April 2017. Downloaded by University of California - San Diego on 29/05/2017 12:10:43.

To illustrate the effect of the TTE DNA template on the growth of fluorescent Cu NPs, the characteristics and optical features of TTE DNA–Cu NPs were investigated and compared with those of **1**–Cu NPs. First, the prepared TTE DNA–Cu NPs (a and b) and **1**–Cu NPs (c and d) were characterized by TEM at different magnifications (Fig. 1C). It showed that the Cu NPs could be successfully generated on both DNA templates. The particle size distribution showed that the average size of TTE DNA–Cu NPs and **1**–Cu NPs increased from 2.3 to 6.3 nm and 2.0 to 6.0 nm (insets of a and c in Fig. 1C), respectively. Through the calculation of the frequency distribution histogram of TTE DNA–Cu NPs and **1**–Cu NPs, the overall standard deviations were found to be 10.94 and 14.63, respectively, which indicated that the discrete characteristic of **1**–Cu NPs was greater than that of TTE DNA–Cu NPs. In addition, from TEM images with different magnifications, it was observed that the average distance between the Cu NPs generated on TTE DNA was smaller than that on DNA 1, indicating TTE DNA–Cu NPs were more aggregated than **1**–Cu NPs. Besides the size and distance, the shape of TTE DNA–Cu NPs was also found to be more uniform than **1**–Cu NPs from the TEM images. Thus, it was suggested that TTE DNA might be more propitious to the growth of Cu NPs.

Furthermore, by monitoring the fluorescence spectra (Fig. 1D), it was observed that the emission of both TTE DNA–Cu NPs and **1**–Cu NPs appeared at 615 nm (curves a and b) and excitation at 340 nm and the spectral shape remained nearly unchanged, which were the characteristics of the excitation/emission spectra of polyT–Cu NPs according to the literature. However, the fluorescence intensity of the Cu NPs grown on the crowded DNA structure (TTE, curve a) was about twice higher than that on the non-crowded structure (DNA 1, curve b). The inset of Fig. 1D also shows that TTE DNA–Cu NPs exhibited a more visibly red fluorescence brighter than **1**–Cu NPs under a UV lamp. Further, these fluorescent Cu NPs were explored by measuring the photoluminescence absolute quantum yields (AQYs) based on the use of a commercially available fluorimeter and an integrating sphere. The AQY of TTE DNA–Cu NPs is 4.7% (relative to MOPS buffer) greater than 3.9% of **1**–Cu NPs. This indicated that the TTE DNA structure was favorable for the fluorescence enhancement of Cu NPs. On the other hand, Fig. 1E shows that the absorption spectrum of TTE DNA–Cu NPs (curve a) changed only slightly compared with **1**–Cu NPs (curve b) and the intensity upon maximum absorption of TTE DNA–Cu NPs was even lower than **1**–Cu NPs. These implied that the enhanced fluorescence emission and quantum yield were not due to the formation of more Cu NPs, but maybe due to the TTE crowded structure.

Since the characterization showed that the crowded TTE DNA structure was favorable for the enhanced fluorescence of Cu NPs, the effect of the crowding extent on the fluorescence of Cu NPs was further studied. The regulation of the crowding extent in the loop part for the growth of Cu NPs was realized in two ways: (1) different numbers of cytosine (C) (0, 5, 10 and 15) were designed next to the T bases of the polyT region (denoted as (1), (2), (3) and (4) TTE DNA) to create different spaces in the loop; and (2) different complementary base pairs were designed to obtain tied parts (double-helical section) with different lengths. As shown in Fig. 2A and B, the prepared (1), (2), (3) and (4) TTE DNA–Cu NPs in the loop part were investigated using TEM and fluorescence spectra. With the gradual increase in the

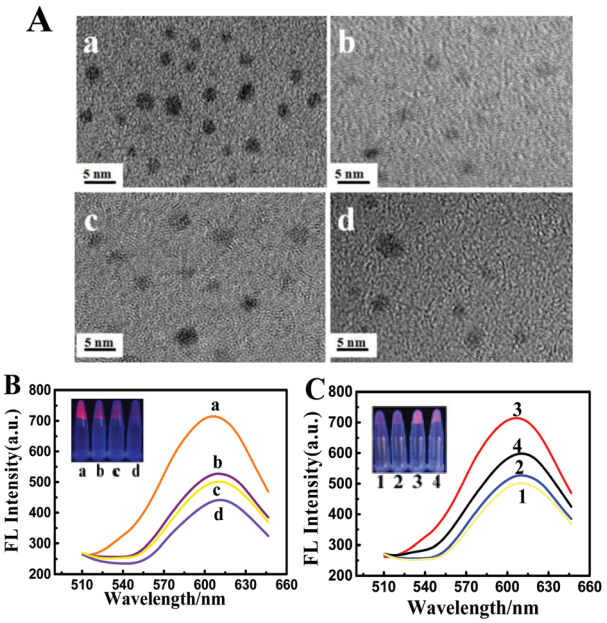

Fig. 2 (A) TEM images of Cu NPs on (1), (2), (3) and (4) TTE DNA with 0, 5, 10, and 15 C bases linking polyT; fluorescence emission of the λ_{ex} = 340 nm/λ_{em} = 615 nm bands of fluorescent Cu NPs synthesized on (1), (2), (3) and (4) TTE DNA–Cu NPs (curves a, b, c and d) (B) and TTE DNA templates with 10, 20, 30 and 40 base pairs (curves 1, 2, 3 and 4) in the duplex part (C). Insets: The corresponding fluorescent Cu NPs generated under UV-light excitation.

number of C bases near to polyT in the loop region, enlarging the growing space of Cu NPs, the distance between particles became gradually larger and the intensity of the fluorescence signal decreased gradually. The corresponding fluorescent Cu NPs were observed under the UV lamp (Fig. 2B inset), clearly showing that (1) TTE DNA–Cu NPs were brighter red than (2), (3) and (4) TTE DNA–Cu NPs. Furthermore, the fluorescence intensity of Cu NPs grown on the TTE DNA structure with different base pairs in the tied part was also studied. As shown in Fig. 2C, the fluorescence signal intensified with the increase in tied base pairs from 10 to 30. It may be because a longer tied section was favorable for creating a more stable and crowded space for the growth of TTE DNA–Cu NPs. However, when the complementary pairing bases in the double-helical section were increased to 40, the fluorescence intensity of the formed Cu NPs weakened. The corresponding Cu NPs were observed under the UV lamp (Fig. 2C inset). A possible reason was that a too long tied section would cause interference to the comfortable growth of Cu NPs. Therefore, it was suggested that suitable duplexes in two ends and smaller spaces in the loop caused more crowded room for favorable growth of Cu NPs.

Herein, an effective combination of the enhanced fluorescence of TTE DNA–Cu NPs, with an easily available exonuclease III (exo III)[19] and an ideal biocatalyst, Zn^{2+}-dependent DNAzyme,[20] assisted target recycling amplification, was explored for ultrasensitive detection of sequence-specific nucleic acids for the first time (Scheme S1 with a detailed description provided in the ESI†).

To verify the feasibility of the proposed assay strategy, fluorescent signals obtained upon analyzing the target DNA and those in a series of control experiments are depicted in Fig. S1 (ESI†). Under optimized experimental conditions (Fig. S2, ESI†), the analytical

Published on 26 April 2017. Downloaded by University of California - San Diego on 29/05/2017 12:10:43.

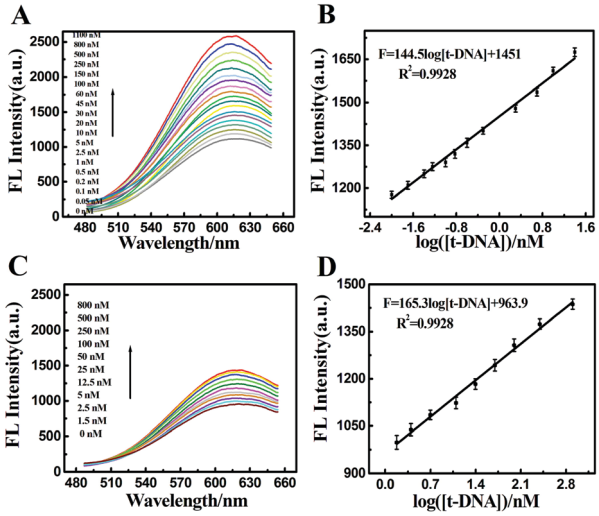

Fig. 3 Fluorescence spectra (A and C) and linear relationship between the fluorescence intensity and the logarithmic concentrations (B and D) using TTE DNA–Cu NPs with dual-cycle amplification and control experiments upon analyzing different concentrations of the target DNA from 0 to 1100 nM (A) and 0 to 800 nM (C), respectively (from bottom to top). Error bars represent standard deviations of measurements (n = 3).

performance of TTE DNA–Cu NPs with a dual amplification-based fluorescence biosensing platform was investigated towards target DNA under gradient concentrations. As shown in Fig. 3A, it was found that the fluorescence intensity gradually increased with increasing concentration of target DNA. Fig. 3B shows the relationship between the DNA concentration and the fluorescence intensity at the maximum emission wavelength (615 nm). The fluorescence intensity exhibited a linear correlation with the logarithm of target DNA concentration from 0.01 to 10 nM. The correlation equation was $F = 144.5 \log_{10}{}^{[\text{target 1DNA}]} + 1451$ ($R^2 = 0.9928$) and the detection limit of target DNA (3δ/slope) was approximately 3 pM. A control experiment was also conducted (Scheme S2, ESI†). As can be seen, the fluorescence intensity also gradually increased with increasing concentration of target DNA (Fig. 3C) with a detection limit corresponding to 0.5 nM (3δ/slope) and a calibration function of $F = 165.3 \log_{10}{}^{[\text{target DNA}]} + 963.9$ ($R^2 = 0.9928$) (Fig. 3D). The higher detection limit confirmed that the TTE DNA–Cu NP based dual-cycle amplification was superior to conventional polyT DNA–Cu NPs. The sequence discrimination of the autocatalytic dual-cycle amplification and sample amplifications were investigated and are shown in Fig. S3 and Table S3 (ESI†).

In this communication, we presented the first attempt to find a crowded TTE DNA structure for the low-cost and convenient preparation of Cu NPs with a great improvement in the fluorescence intensity compared to conventional polyT–Cu NPs. The TTE DNA template changes the Cu NPs' growing environment by diversifying the structure of the DNA, avoiding the complicated synthesis or extending the chain of DNA. As a proof of concept, a protocol based on TTE DNA–Cu NPs with an autocatalytic dual-cycle amplification strategy was developed for the detection of target specific sequence DNA with high sensitivity and selectivity. It is the first time that TTE DNA–Cu NPs have been constructed and applied in a biosensor. We posit that this strategy by regulating the DNA crowding extent will open up a new way for enhancing the fluorescence of DNA–metal nanoparticles and a label-free, efficient and cost-effective fluorescent biosensor could be extended to sensitive detection of other sequence-specific DNAs or proteins by simply changing the corresponding recognition which may have great potential applications in clinical diagnosis and biomedical fields.

This work was financially supported by the projects (No. 21005001, 21675001 and 21371007) from the National Natural Science Foundation of China, the Anhui Provincial Natural Science Foundation (1608085MB46), the Anhui Provincial Education Department Natural Sciences Key Fund (gxyqZD2016023) and the Key Program in the Youth Elite Support Plan in Universities of Anhui Province (gxyqZD2016023).

Notes and references

1 K. E. Sapsford, W. R. Algar and L. Berti, *et al.*, *Chem. Rev.*, 2013, **113**, 1904–2074.
2 (*a*) T. A. C. Kennedy, J. L. MacLean and J. Liu, *Chem. Commun.*, 2012, **48**, 6845–6847; (*b*) Y. Teng, X. Jia and J. Li, *et al.*, *Anal. Chem.*, 2015, **87**, 4897–4902.
3 (*a*) C. I. Richards, S. Choi and J. C. Hsiang, *et al.*, *J. Am. Chem. Soc.*, 2008, **130**, 5038–5039; (*b*) N. Enkin, F. Wang and E. Sharon, *et al.*, *ACS Nano*, 2014, **8**, 11666–11673.
4 (*a*) A. Rotaru, S. Dutta and E. Jentzsch, *et al.*, *Angew. Chem., Int. Ed.*, 2010, **49**, 5665–5667; (*b*) Z. Qing, X. He and D. He, *Angew. Chem., Int. Ed.*, 2013, **52**, 9719–9722.
5 (*a*) Y. H. Hu, Y. M. Wu and T. T. Chen, *et al.*, *Anal. Methods*, 2013, **5**, 3577–3581; (*b*) L. L. Zhang, J. J. Zhao and H. Zhang, *et al.*, *Biosens. Bioelectron.*, 2013, **44**, 6–9; (*c*) L. L. Zhang, J. J. Zhao and M. Duan, *et al.*, *Anal. Chem.*, 2013, **85**, 3797–3801; (*d*) H. B. Wang, H. D. Zhang and Y. Chen, *et al.*, *Biosens. Bioelectron.*, 2015, **74**, 581–586; (*e*) H. Zhang, Z. H. Lin and X. G. Su, *Talanta*, 2015, **131**, 59–63.
6 F. Z. Xu, H. Shi and X. X. He, *et al.*, *Anal. Chem.*, 2014, **86**, 6976–6982.
7 (*a*) C. X. Song, X. H. Yang and K. M. Wang, *et al.*, *Anal. Chim. Acta*, 2014, **827**, 74–79; (*b*) J. Zhao, S. S. Hu and Y. Cao, *et al.*, *Biosens. Bioelectron.*, 2015, **66**, 327–331.
8 Y. Zhang, Z. W. Chen and Y. Tao, *et al.*, *Chem. Commun.*, 2015, **51**, 11496–11499.
9 Q. W. Song and Y. Shi, *et al.*, *Chem. – Eur. J.*, 2015, **21**, 2417–2422.
10 Z. H. Qing, X. X. He and T. P. Qing, *et al.*, *Anal. Chem.*, 2013, **85**, 12138–12143.
11 Z. G. Mao, Z. H. Qing and T. P. Qing, *et al.*, *Anal. Chem.*, 2015, **87**, 7454–7460.
12 (*a*) L. J. Ou and X. Y. Li, *et al.*, *Analyst*, 2015, **140**, 1871–1875; (*b*) L. J. Ou, X. Y. Li and H. W. Liu, *et al.*, *Anal. Sci.*, 2014, **30**, 723–727.
13 (*a*) H. B. Wang, H. D. Zhang and Y. Chen, *et al.*, *Anal. Methods*, 2015, **7**, 6372; (*b*) H. B. Wang, H. D. Zhang and Y. Chen, *et al.*, *Biosens. Bioelectron.*, 2015, **74**, 581–586; (*c*) H. B. Wang, Y. Chen and Y. Li, *et al.*, *RSC Adv.*, 2015, **5**, 94099–94104.
14 J. Y. Li, L. Si and J. C. Bao, *et al.*, *Anal. Chem.*, 2017, **89**, 3681–3686.
15 Y. N. Wang, H. Y. Cui and Z. J. Cao, *Talanta*, 2016, **154**, 574–580.
16 (*a*) H. X. Zhou, G. Rivas and A. P. Minton, *Annu. Rev. Biophys.*, 2008, **37**, 375–397; (*b*) M. H. Kombrabail and G. Krishnamoorthy, *J. Fluoresc.*, 2005, **15**, 741; (*c*) D. Miyoshi, A. Nakao and N. Sugimoto, *Biochemistry*, 2002, **41**, 15017–15024; (*d*) D. Miyoshi and N. Sugimoto, *Biochimie*, 2008, **90**, 1040; (*e*) R. Moriyama, Y. Iwasaki and D. Miyoshi, *J. Phys. Chem. B*, 2015, **119**, 11969–11977; (*f*) S. I. Nakano, D. Miyoshi and N. Sugimoto, *Acids Chem. Rev.*, 2014, **114**, 2733–2758.
17 (*a*) A. Zaki, N. Dave and J. W. Liu, *J. Am. Chem. Soc.*, 2012, **134**, 35; (*b*) Y. Xue, Z. Y. Kan and Q. Wang, *et al.*, *J. Am. Chem. Soc.*, 2007, **129**, 11185–11191; (*c*) M. Kellner and M. Heidrich, *Sci. Rep.*, 2016, **6**, 35606.
18 J. N. Zadeh, C. D. Steenberg and J. S. Bois, *et al.*, *J. Comput. Chem.*, 2011, **32**, 170–173.
19 (*a*) F. Xuan, X. Luo and I. M. Hsing, *Anal. Chem.*, 2012, **84**, 5216–5220; (*b*) H. J. Lee, Y. Li, A. W. Wark and R. M. Corn, *Anal. Chem.*, 2005, **77**, 5096–5100.
20 M. M. Ali and Y. Li, *Angew. Chem., Int. Ed.*, 2009, **48**, 3512–3515.

 This journal is © The Royal Society of Chemistry 2017